

Focusing of Spin Polarization in Semiconductors by Inhomogeneous Doping

Yuriy V. Pershin and Vladimir Privman

Center for Quantum Device Technology, Clarkson University, Potsdam, New York 13699-5720, USA

(Received 25 February 2003; published 23 June 2003)

We study the evolution and distribution of nonequilibrium electron spin polarization in n -type semiconductors within the two-component drift-diffusion model in an applied electric field. Propagation of spin-polarized electrons through a boundary between two semiconductor regions with different doping levels is considered. We assume that inhomogeneous spin polarization is created locally and driven through the boundary by the electric field. We show that an initially created narrow region of spin polarization can be further compressed and amplified near the boundary. Since the boundary involves variation of doping but no real interface between two semiconductor materials, no significant spin polarization loss is expected. The proposed mechanism will be therefore useful in designing new spintronic devices.

DOI: 10.1103/PhysRevLett.90.256602

PACS numbers: 72.25.Dc, 72.20.Ht, 72.25.Hg, 72.25.Mk

Introduction.—Theoretical and experimental investigations of spin-related effects in semiconductors have received much attention recently [1–5] owing to the proposals for devices based on manipulation of electron spin [6–16]. Operation of a spintronic device requires efficient spin injection into a semiconductor, spin manipulation, control and transport, and also spin detection. Once injected into a semiconductor, electrons experience spin-dependent interactions with the environment, which cause relaxation. Because of diffusion, spin polarization spreads over the sample and spin polarization density decreases as well. For effective spin manipulation and detection, it is desirable to have high spin polarization densities—the problem addressed in the present Letter.

Nonequilibrium spin polarization can be introduced into a semiconductor in various ways. Experimentally, it is realizable at the interface between semiconductor and ferromagnetic metal or magnetic semiconductor [17,18], or by using optical pumping techniques [19–21]. Another possible approach is to use hyperfine interaction of electrons with polarized nuclei [22]. In the latter scheme, the nuclear spins should be first polarized by optical pumping, or by spin-polarized current [7,23,24], or (anti)ferromagnetically ordered at ultralow temperatures [25]. In this work, we consider spin polarization created locally in the bulk of semiconductor, for example, by using ferromagnetic-metal scanning tunneling microscopy tips [26,27], or by optical pumping techniques [19–21].

Figure 1 shows the system under investigation. Localized electron spin polarization is created by a source in the semiconductor region with the doping density N_1 . Under influence of the applied electric field, the spin-polarized carriers drift through the boundary between the two semiconductor regions, i.e., from the region with the doping density N_1 to the region with the doping density N_2 . It is assumed that $N_2 \geq N_1$. In our calculations, we use the two-component drift-diffusion model

[28,29], and we take into account the effects of the charge accumulation/redistribution near the boundary. The latter effect is analogous to the depletion region formation in a p - n junction [30], and it introduces a coordinate-dependent electric field in the equation for the spin polarization density. We solve the resulting differential equations for the electric field and spin polarization density numerically. Two types of spin polarization source are considered: instantaneous source and continuous one. The main result of our calculations is that the spin polarization density can be condensed and amplified near the boundary. The system of interest does not require a real interface between semiconductor materials. We only assume variation in the doping level. Therefore, additional electron spin polarization losses at interfaces [31] can be avoided. This result will be useful in designing new spintronic devices.

Model.—Our theoretical investigation is based on the two-component drift-diffusion model (see, e.g., [29]). In our case, the system is described by the following set of equations:

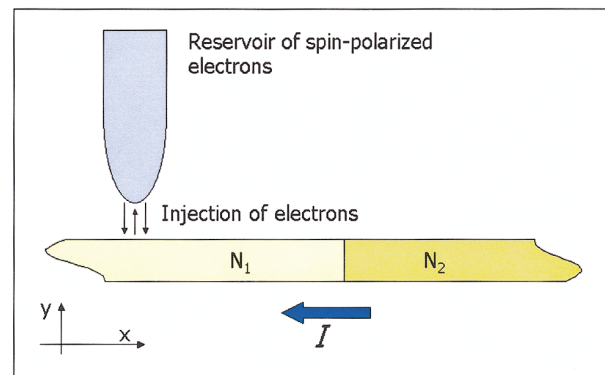


FIG. 1 (color). Injection of spin-polarized electrons in a system with two levels of doping.

$$e \frac{\partial n_{\uparrow(\downarrow)}}{\partial t} = \text{div} \vec{j}_{\uparrow(\downarrow)} + \frac{e}{2\tau_{sf}} (n_{\uparrow(\downarrow)} - n_{\downarrow(\uparrow)}) + S_{\uparrow(\downarrow)}(\vec{r}, t), \quad (1)$$

$$\vec{j}_{\uparrow(\downarrow)} = \sigma_{\uparrow(\downarrow)} \vec{E} + eD \nabla n_{\uparrow(\downarrow)}, \quad (2)$$

and

$$\sigma_{\uparrow(\downarrow)} = e n_{\uparrow(\downarrow)} \mu, \quad (3)$$

where $-e$ is the electron charge, $n_{\uparrow(\downarrow)}$ is the density of spin-up (spin-down) electrons, $\vec{j}_{\uparrow(\downarrow)}$ is the current density, τ_{sf} is the spin relaxation time, $S_{\uparrow(\downarrow)}(\vec{r}, t)$ describes the source of the spin polarization, $\sigma_{\uparrow(\downarrow)}$ is the conductivity, and μ is the mobility, connected with the diffusion coefficient D via the Einstein relation $\mu = De/(k_B T)$, and defined via $\vec{v}_{\text{drift}} = \mu \vec{E}$.

Equation (1) is the usual continuity relation that takes into account spin relaxation and the source of the spin polarization, Eq. (2) is the expression for the current which includes the drift and diffusion contributions, and Eq. (3) is the expression for the conductivity. It is assumed that the diffusion coefficient D and the spin relaxation time τ_{sf} are equal for spin-up and spin-down electrons.

To separate the equations for the charge and spin degrees of freedom, we introduce the charge density $n = n_{\uparrow} + n_{\downarrow}$ and the spin polarization density $P = n_{\uparrow} - n_{\downarrow}$. The charge density is described by the equations

$$\vec{j}_0 = e n \mu \vec{E} + eD \nabla n, \quad (4)$$

and

$$\text{div} \vec{E} = \frac{e}{\epsilon \epsilon_0} (N_i - n). \quad (5)$$

Here \vec{j}_0 is the current flowing through the sample, ϵ_0 is the permittivity of free space, and ϵ is the dielectric constant. We assume that at room temperature the density of the ionized donors N_i is equal to the donor density ($N_i = N_1$ for $x < 0$ and $N_i = N_2$ for $x > 0$); i.e., all the donors are ionized. Equation (4) was obtained from Eqs. (1)–(3) by neglecting the term which describes the source of the spin polarization, because we have assumed that charge equilibration processes at the point of injection do not significantly influence the electric field profile and thus the propagation of the spin polarization through the boundary. Relation (5) is the Poisson equation. Combining Eqs. (4) and (5), we obtain the equation describing the electric field distribution,

$$\frac{\partial^2 E}{\partial x^2} + \frac{e}{kT} E \frac{\partial E}{\partial x} - \frac{e^2 N_i}{kT \epsilon \epsilon_0} E = -\frac{j_0}{\epsilon \epsilon_0 D} + \frac{e}{\epsilon \epsilon_0} \nabla N_i, \quad (6)$$

where E is in the x direction.

The electric field distribution can be found from Eq. (6) as a function of the current j_0 through the sample. The current as the external control parameter, rather than the applied voltage, is more convenient because the current is

constant throughout the electric circuit that contains the sample. If we use the voltage as the external control parameter, we have to take into account voltage drops in different parts of the circuit, such as, for example, at the Schottky barriers between metal and semiconductor.

From the set of relations (1)–(3), we obtain an equation for the spin polarization density,

$$\frac{\partial P}{\partial t} = D \Delta P + D \frac{e \vec{E}}{k_B T} \nabla P + D \frac{e \nabla \vec{E}}{k_B T} P - \frac{P}{\tau_{sf}} + F(\vec{r}, t). \quad (7)$$

Here $F(\vec{r}, t) = [S_{\uparrow}(\vec{r}, t) - S_{\downarrow}(\vec{r}, t)]/e$ represents the spin polarization density created by the external source. The spin polarization density is coupled to the charge density through the electric field. Thus, our numerical calculation involves two steps: First, the electric field profile is found as the solution of Eq. (6) and, second, Eq. (7) is solved for the spin polarization density.

Results and discussion.—To proceed with the solution of Eq. (6), let us introduce the dimensionless variables as $\tilde{E} = E/E_0$ and $\tilde{x} = x/x_0$, where $E_0 = j_0 kT/(DN_1 e^2)$ and $x_0^{-2} = e^2 N_1/(kT \epsilon \epsilon_0)$. Equation (6) can be rewritten as

$$\frac{\partial^2 \tilde{E}}{\partial \tilde{x}^2} + \alpha \tilde{E} \frac{\partial \tilde{E}}{\partial \tilde{x}} - \frac{N_i}{N_1} \tilde{E} + 1 - \beta \delta(\tilde{x}) = 0, \quad (8)$$

where $\alpha = x_0 E_0 e/kT$ and $\beta = x_0 e(N_2 - N_1)/(E_0 \epsilon \epsilon_0)$. Estimation of the dimensionless constant α and of x_0 , for $E = 10^3$ V/cm and $N_1 = 10^{15}$ cm $^{-3}$, gives $x_0 = 1.37 \times 10^{-7}$ m and $\alpha = 0.52$. The solution of Eq. (8) was found numerically. Figure 2 shows the electric field profile near the boundary for the selected parameter values.

It is also convenient to rewrite Eq. (7) in the dimensionless form. With the dimensionless variables selected

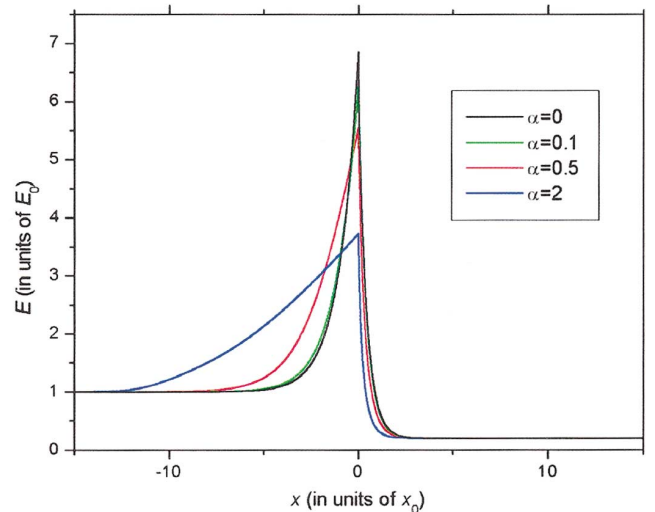


FIG. 2 (color). Electric field profile near the boundary, $N_2/N_1 = 5$, $\beta = -19$.

as follows, $\tau = t/\tau_{sf}$, $X = x/x_1$, with $x_1 = \sqrt{D\tau_{sf}}$, we get

$$\frac{\partial p}{\partial \tau} = \frac{\partial^2 p}{\partial X^2} + \sqrt{D\tau_{sf}} \frac{e}{k_B T} \left(E \frac{\partial p}{\partial X} + p \frac{\partial E}{\partial X} \right) - p + g. \quad (9)$$

The source function g and dimensionless spin polarization density are defined for instantaneous and continuous sources in different ways. Assuming an instantaneous source, we take the function F in Eq. (7) as $F = F_0 f(x) \delta(t)$, with $f(x)$ normalized to 1; then, $g = x_1 f(X) \delta(\tau)$ and $p = P x_1 / F_0$. Here F_0 measures the spin polarization density created at the initial moment of time. The continuous source $F = G_0 \delta(x)$ is described by the constant G_0 , which measures the spin polarization density created per unit time. The dimensionless polarization density in this case is defined as follows: $p = P x_1 / F_0 \tau_{sf}$, with $g = \delta(X)$.

We have solved Eq. (9) numerically, for different values of the parameters. The obtained spin polarization density profiles are qualitatively similar. The results presented here, calculated for a selected typical set of parameter values, are representative of the general idea of our proposal. Evolution of the spin polarization density created at $t = 0$ by the instantaneous source is shown in Fig. 3. We have selected the profile of initial spin polarization in the Gaussian form and solved Eq. (9) using an iterative scheme. Under influence of the electric field, the spin polarization density profile moves towards the boundary. Its width increases due to diffusion, and the amplitude decreases due to the combined action of the different spin relaxation mechanisms and diffusion processes. As the spin polarization density profile approaches the boundary, its velocity increases. It reaches the maximum at the boundary, where the electric field is maximal. In the region with higher donor density, N_2 , the electric field is lower, and the velocity of the spin polar-

ization profile decreases. As a result, the spin polarization gathers in a narrow spatial region (Fig. 3).

The spin polarization corresponding to $\tau = 0.11$, in Fig. 3, still represents a dynamical solution of Eq. (9). However, at such late times, the velocity of the spin polarization profile is much lower, at least by a factor N_1/N_2 , than at earlier times, when the spin polarization density was concentrated mainly in the first semiconductor or in the interface region. Thus, the peaked spin polarization profile at $\tau = 0.11$ can be regarded as quasi-static, its position and amplitude slowly varying in time. After a long time, it will dissipate due to spin relaxation and diffusion processes. Figure 4 shows the equilibrium solutions of Eq. (9) with the continuous source of spin polarization for different values of the doping density. If the doping densities are equal ($N_1 = N_2$), then the spin polarization density decreases monotonically with distance from the injection point. The peak value of the spin polarization density, past the boundary, increases as the doping density increases.

Physically, the mechanism of the spin polarization density amplification near the boundary at which the doping is changed can be understood as follows. The spin polarization density can be increased near the boundary due to the charge localization: In the N_2 semiconductor region, the density of the electrons must be high. The electrons moving fast in the N_1 region, then move slowly in the N_2 region, and gather in a small spatial region near the boundary.

Conclusions.—Electron spin transport through the boundary between two semiconductor regions with different doping levels could lead to the electron spin polarization amplification near the boundary. The built-in electric field at the boundary accelerates propagation of the spin polarization through the boundary, if spin

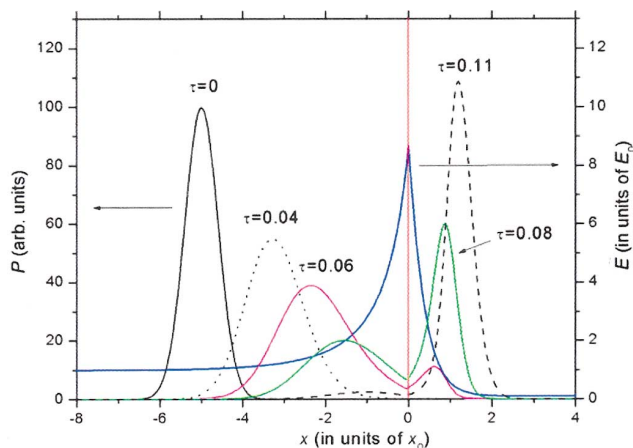


FIG. 3 (color). Dynamics of propagation through the boundary of spin-polarized electrons injected at $\tau = 0$, where $\tau = t/\tau_{sf}$, for $N_2/N_1 = 10$. The blue curve denotes the electric field. The other curves show the distribution of the spin polarization density at different times.

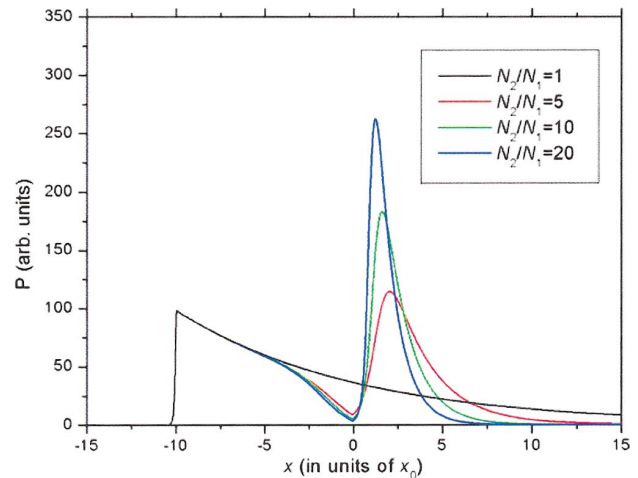


FIG. 4 (color). Distribution of the spin polarization density created by a point source located at $x = -10$. Spin accumulation effect near the boundary becomes more pronounced with increased N_2 .

polarization passes from the low doping region to the high doping region. Spin amplification occurs past the boundary, within the distance of the order of the depletion layer width. It must be emphasized that there exists other mechanisms allowing increasing spin polarization density near a boundary. For example, the two semiconductor regions could have different diffusion coefficients; for a more efficient spin focusing near the boundary, a lower diffusion coefficient of the N_2 region would be desirable. However, as mentioned in the introduction, the mechanism considered here, involving only the doping variation, has the advantage of not requiring a materials interface, thus avoiding additional spin polarization losses.

We gratefully acknowledge helpful discussions with Professor M.-C. Cheng and Professor V.N. Gorshkov. This research was supported by the National Science Foundation, Grants No. DMR-0121146 and No. ECS-0102500, and by the National Security Agency and Advanced Research and Development Activity under Army Research Office Contract No. DAAD 19-02-1-0035.

-
- [1] G. Prinz, *Science* **282**, 1660 (1998).
- [2] S. A. Wolf, D. D. Awschalom, R. A. Buhrman, J. M. Daughton, S. von Molnár, M. L. Roukes, A. Y. Chtchelkanova, and D. M. Treger, *Science* **294**, 1488 (2001).
- [3] S. Das Sarma, J. Fabian, X. Hu, and I. Zutic, *IEEE Trans. Magn.* **36**, 2821 (2000).
- [4] S. Das Sarma, *Am. Sci.* **89**, 516 (2001).
- [5] D. D. Awschalom, M. E. Flatte, and N. Samarth, *Sci. Am.* **286**, 66 (2002).
- [6] S. Datta and B. Das, *Appl. Phys. Lett.* **56**, 665 (1990).
- [7] B. E. Kane, L. N. Pfeiffer, and K. W. West, *Phys. Rev. B* **46**, 7264 (1992).
- [8] M. Johnson, *Science* **260**, 320 (1993).
- [9] M. E. Flatte and G. Vignale, *Appl. Phys. Lett.* **78**, 1273 (2001).
- [10] I. Zutic, J. Fabian, and S. Das Sarma, *Appl. Phys. Lett.* **79**, 1558 (2001).
- [11] C. Ciuti, J. P. McGuire, and L. J. Sham, *Appl. Phys. Lett.* **81**, 4781 (2002).
- [12] T. Koga, J. Nitta, and H. Takayanagi, *Phys. Rev. Lett.* **88**, 126601 (2002).
- [13] X. F. Wang, P. Vasilopoulos, and F. M. Peeters, *Phys. Rev. B* **65**, 165217 (2002).
- [14] R. G. Mani, W. B. Johnson, V. Narayanamurti, V. Privman, and Y.-H. Zhang, *Physica (Amsterdam)* **12E**, 152 (2002).
- [15] J. Schliemann, J. C. Egues, and D. Loss, *Phys. Rev. Lett.* **90**, 146801 (2003).
- [16] I. Žutić, J. Fabian, and S. Das Sarma, *Phys. Rev. B* **66**, 165301 (2002).
- [17] J. Nitta, T. Akazaki, H. Takayanagi, and T. Enoki, *Phys. Rev. Lett.* **78**, 1335 (1997).
- [18] G. Meir, T. Matsuyama, and U. Merkt, *Phys. Rev. B* **65**, 125327 (2002).
- [19] J. M. Kikkawa and D. D. Awschalom, *Phys. Rev. Lett.* **80**, 4313 (1998).
- [20] J. M. Kikkawa and D. D. Awschalom, *Nature (London)* **397**, 139 (1999).
- [21] D. Hägele, M. Oestreich, W. W. Rühle, N. Nestle, and K. Eberl, *Appl. Phys. Lett.* **73**, 1580 (1998).
- [22] Yu. V. Pershin and V. Privman, *Nano Lett.* **3**, 695 (2003).
- [23] K. R. Wald, L. P. Kouwenhoven, P. McEuen, N. C. van der Vaart, and C. T. Foxon, *Phys. Rev. Lett.* **73**, 1011 (1994).
- [24] D. C. Dixon, K. R. Wald, P. L. McEuen, and M. R. Melloch, *Phys. Rev. B* **56**, 4743 (1997).
- [25] S. Rehmann, T. Herrmannsdörfer, and F. Pobell, *Phys. Rev. Lett.* **78**, 1122 (1997).
- [26] S. F. Alvarado and P. Renaud, *Phys. Rev. Lett.* **68**, 1387 (1992).
- [27] S. F. Alvarado, *Phys. Rev. Lett.* **75**, 513 (1995).
- [28] Z. G. Yu and M. E. Flatté, *Phys. Rev. B* **66**, 235302 (2002).
- [29] Z. G. Yu and M. E. Flatté, *Phys. Rev. B* **66**, 201202 (2002).
- [30] S. M. Sze, *Semiconductor Devices: Physics and Technology* (Wiley, New York, 1985).
- [31] J. T. Olesberg, Wayne H. Lau, Michael E. Flatté, C. Yu, E. Altunkaya, E. M. Shaw, T. C. Hasenberg, and Thomas F. Boggess, *Phys. Rev. B* **64**, 201301 (2001).